land

MDPI

Article

Classifying Slope Unit by Combining Terrain Feature Lines Based on Digital Elevation Models

Hao Wang [1,2,3], Guanghui Hu [1,2,3], Junfei Ma [1,2,3], Hong Wei [1,2,3], Sijin Li [1,2,3], Guoan Tang [1,2,3] and Liyang Xiong [1,2,3,*]

[1] School of Geography, Nanjing Normal University, Nanjing 210023, China
[2] Key Laboratory of Virtual Geographic Environment, Ministry of Education, Nanjing Normal University, Nanjing 210023, China
[3] Jiangsu Center for Collaborative Innovation in Geographical Information Resource Development and Application, Nanjing Normal University, Nanjing 210023, China
* Correspondence: xiongliyang@njnu.edu.cn

Abstract: In recent years, applications and analyses based on slope units have become increasingly widespread. Compared with grid units, slope units can better represent terrain features and boundaries and allow a more complete view of the morphology of the Earth's surface. Maps based on slope units also offer significant improvements for disaster prediction and the analysis of slope land resources. Therefore, we need a reasonable method of slope unit classification. Although some methods have been proposed for slope unit classification, they have been too focused on morphological variations and have not fully considered the importance of geomorphology, and the geomorphological and physical significance of slope partitioning remain unclear. Therefore, we propose a novel slope unit classification method by combining terrain feature lines (CTFL) derived from the meaning of geomorphology ontology that use several terrain feature lines, such as geomorphic water division lines, valley shoulder lines, slope toe lines, and shady/sunny slope boundary lines, to classify slopes. The Jiuyuangou and Lushan study areas were selected to test the CTFL method. Compared with the traditional hydrological method, the CTFL method can effectively overcome topographic abruptness and distortions, improve the uniformity of slope and aspect within individual units, and increase the accuracy of slope unit applications and analyses. This work fully considers the importance of geomorphology and is conducive to future studies of slope unit division.

Keywords: terrain features; geomorphology; homogeneity; sloping land resources; DEM

Citation: Wang, H.; Hu, G.; Ma, J.; Wei, H.; Li, S.; Tang, G.; Xiong, L. Classifying Slope Unit by Combining Terrain Feature Lines Based on Digital Elevation Models. *Land* **2023**, *12*, 193. https://doi.org/10.3390/land12010193

Academic Editor: Giulio Iovine

Received: 2 December 2022
Revised: 2 January 2023
Accepted: 3 January 2023
Published: 6 January 2023

1. Introduction

The Earth's surface is undulating, rugged, and varied [1]. This ruggedness can be both continuous and discontinuous and is marked by abrupt, constant, and gradual changes. In present, for the representations of the Earth's surface, sometimes small regions [2,3] or grid units are adopted in statistically based [4,5] and physically based models [6–8]. Grid units are favored because of their simpler data structure, which expedites analytical performance on complex data set classes. Additionally, grid units have favorable applicability to the basic assumptions of infinite slope models [9]. However, grid units do not represent the terrain features and boundaries of natural slopes in the real world and do not provide a more complete perspective of the ground surface morphology in our daily lives [10,11]. In contrast, slope units allow a better representation of terrain features and boundaries and overcome some of the drawbacks associated with the use of grid units, hence the increasing use and research on slope units.

Currently, a slope unit is defined as a relatively homogeneous and continuously distributed area divided by hydrographic or other demarcation lines [12–14]. In fact, the use of slope units is very widespread. In addition to being important for landslide prediction, they are also important for the evaluation of resources on sloped land, and because the geomorphological processes within the slope unit are uniformly characterized, maps based on slope units are inherently more suitable for land use planning and disaster management than grid units [15]. The proper delineation of slope units is at the foundation of many terrain analysis applications. A slight error in the delineation of slope units will lead to a decrease in the accuracy of the subsequent analysis and experimental results based on those slope units [16]. Therefore, it is especially important to correctly delineate slope units. Slope units can be drawn manually from topographic maps, but the disadvantages of this method are that it is subjective and that manually extracting slope units is time consuming and only suitable for small areas [17,18]. The most common method of delineating slope units is currently a GIS-based hydrological method, where slope units are extracted by using normal and inverse DEMs as input data and by extracting different subbasins along ridgelines and valley lines and determining their overlap through operations such as flow direction calculations, flow accumulation threshold calculations, stream network extraction, watershed areas, etc. However, the slope units extracted with this method only reflect the general degree of change in the slope along the direction of flow [19,20]. For example, the direction of flow extracted with the D8 algorithm only represents the steepest slope features, while slope changes outside the direction of flow are not well represented, especially near the toe line or along the gully, which poorly expresses the homogeneity of each slope unit [21]. Other scholars divided slope units by utilizing some topographic attributes from the study area (e.g., slope gradient, aspect, curvature, etc.). The differences between these methods focus on how to best utilize the information contained in geomorphometric variables and on the choice of target units of classification. Methods can be divided into those which are cell-based and those that are object-based [22,23]. Methods can be divided into those that use a classifier designed manually on the basis of expert knowledge and empirical evidence [24–26] and those that use a classifier generated by a machine learning algorithm [27,28]. They either divide the slope units only in the attribute domain, ignoring the spatial location information, or their processing methods are too cumbersome, greatly limiting the practicality of the methods. The selection of parameters for these methods is crucial in the division of slope units, and the slightest error in parameterization can result in slope units that are too dense or too sparse; thus, requiring frequent and lengthy trials to determine the appropriate parameters. There is other GIS-based hydrological methods that take into account the homogeneity and the average aspect direction of each terrain portion to divide the slope units [29–31], but they are more suitable for assessing the stability of physics-based slopes of infinite size and artificial slopes using the limit equilibrium method.

The existing methods of classifying slope units are only suitable for specific landscapes, and the units classified by these methods are more or less lacking in geomorphological features. The fundamental reason for these problems is that they do not sufficiently start from the essential definition of the slope unit, lack an effective understanding of the landform, and insufficiently analyze the undulation, genesis mechanism, and distribution of the landform. Geomorphology is a variety of spatial entities on the surface of the earth; it is not an abstract combination of geometric objects but a complex geographic system of spatial properties and relationships [32,33]. Terrain feature elements mainly refer to the points, lines, or surface elements that have a controlling effect on the spatial distribution of features on the surface. Terrain feature elements constitute the basic framework of surface terrain and topographic changes, and their combination determines the basic morphology and geomorphological characteristics of the terrain as well as the property characteristics of the Earth's slope units [34]. At present, with the continuous development of digital elevation models, the methods and techniques of digital terrain analysis are being improved, and the acquisition of terrain feature information is becoming increasingly accurate, while the areas delineated by different terrain feature elements vary in their slope shape, slope position, and slope nature. Moreover, there are various terrain feature lines, and different terrain feature lines represent different geological meanings within the terrain.

Accordingly, this paper proposes a novel slope unit classification method by combining terrain feature lines (CTFL). In this research, the slope units are considered individual slope units formed by the division of terrain feature lines with clear geological significance at the slope scale. These terrain feature lines include geomorphic water dividing lines (ridge lines), valley shoulder lines, slope toe lines, shady/sunny slope boundary lines, and so on. The geological significance of each terrain feature line within the slope division process is explained in detail in Section 2.

2. Materials and Methods

2.1. Data and Study Area

The first study area examined is located in the Jiuyuangou region of Shanxi, China, which is a typical representative catchment in the first subregion of the loess hills and gullies region. This area is characterized by undulating mountains and valleys, fragmented topography, and severe soil erosion. The DEM with a spatial resolution of 5 m is used and encompasses an elevation between 814 m and 1188.3 m [35].

Furthermore, to verify the practicality of the CTFL method with different geomorphological types, the second study area is located in Lushan, Jiangxi, China. This area has a high topography in the northwest and a low topography in the southeast, and the land predominantly consists of mountainous hills. The DEM data with 5 m are used, as shown in Figure 1 [36].

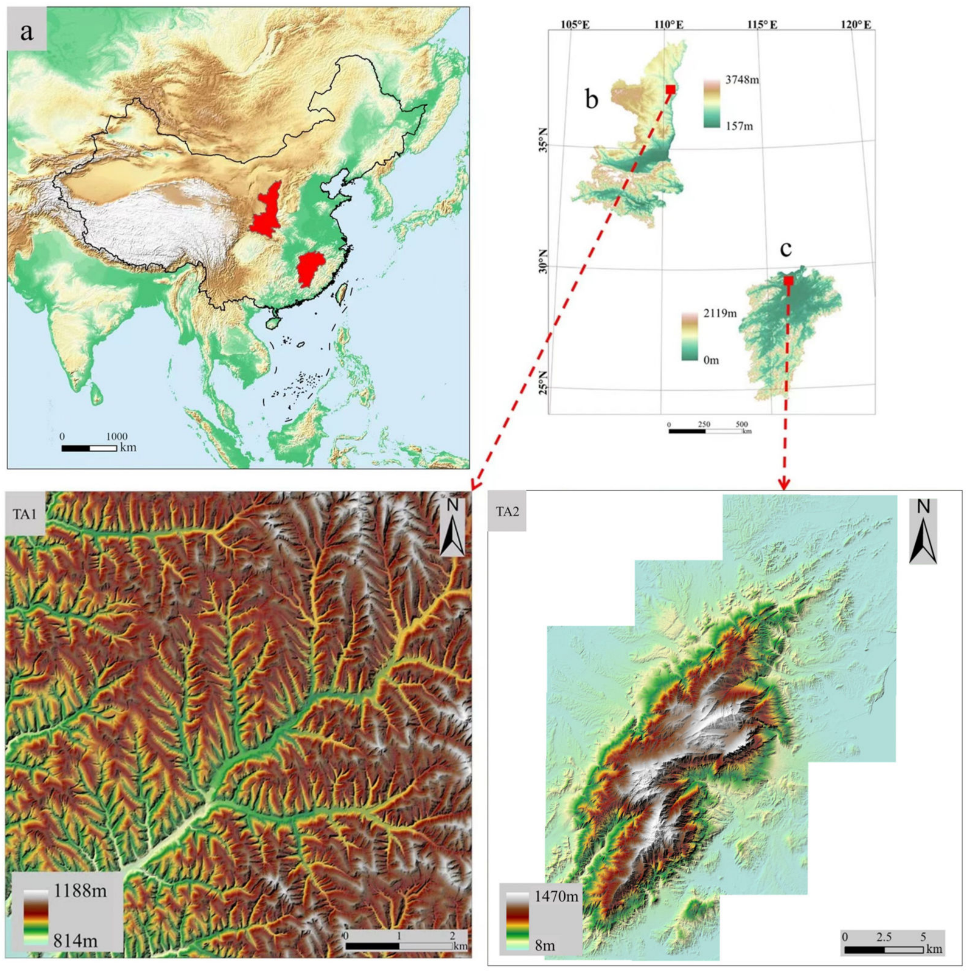

Figure 1. Field study areas: (**a**) the location of study areas (red areas); (**b**) Jiuyuangou area (TA1) in Shanxi Province; (**c**) Lushan area (TA2) in Jiangxi Province.

This research is based on the ArcGIS platform and implemented with the aid of Python programming (Model Builder ArcGIS).

2.2. Slope Unit Classification by Combining Terrain Feature Lines (CTFL)

The first level of division in the CTFL method is the division between ordinary watersheds and inter-watersheds based on the geomorphic water dividing line. On this basis, the abovementioned slope units are divided into positive and negative terrain slope units by using the valley shoulder line, which represents slope units with different slope positions on the surface; furthermore, the negative terrain slope units are divided into gully bottom slope units and non-gully bottom slope units by using the slope toe line. Finally, according to the light exposure characteristics of the slope, the slope units are divided into shady and sunny slope units by using the shady/sunny slope boundary line (the gully bottom is not involved in the division of the shady and sunny slope units). The coding system and combination rules for the CTFL method are shown in Tables 1 and 2, and the general flowchart of the CTFL method is shown in Figure 2.

For the relationship of these four terrain feature lines, which are frequent and important feature lines of different slopes, they all can divide the ground surface into areas with different characteristics to ensure the homogeneity of the final slope unit.

Table 1. The classification coding system of the slope unit.

Fields	Category	Coding
Watershed slope units (x0,000)	Ordinary watershed	10,000
	Inter-watershed	20,000
Positive and negative terrain slope units (0x,000)	Positive terrain	01,000
	Negative terrain	02,000
Gully bottom and non-gully bottom slope units (Is it gully bottom—negative terrain only) (00,x00)	Non-gully bottom (Contains negative terrain non-gully bottom and positive terrain areas)	00,100
	Gully bottom	00,200
Shady and sunny slope units (The bottom of the gully is not divided) (00,0x0)	Sunny slopes	00,010
	Shady slopes	00,020
	Gully bottom slopes (no division)	00,000

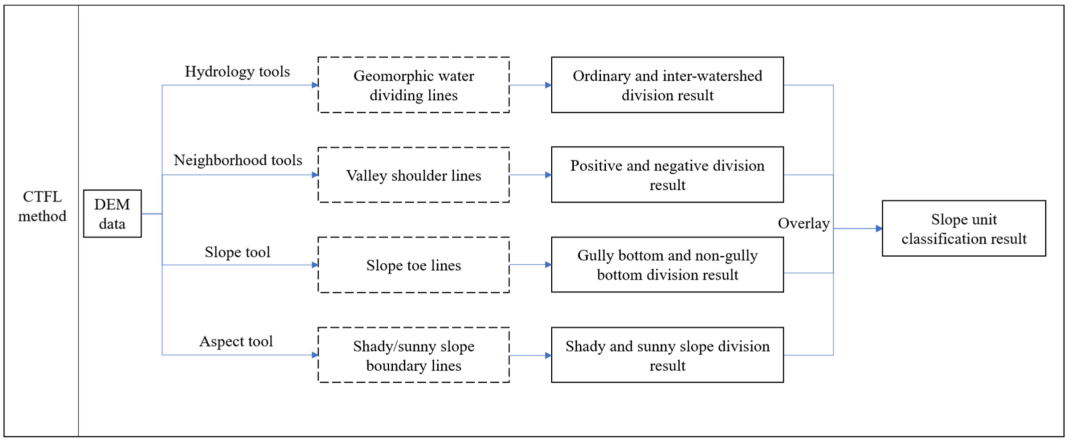

Figure 2. The general flowchart of CTFL method (see Figures 4, 6, and 8 for detailed steps).

Table 2. The combination rules of the CTFL method.

<table>
<tr><th colspan="5">CTFL Method and Their Combination Rules</th></tr>
<tr><th>Rules</th><th>Ordinary Watershed/Inter-Watershed (x0,000)</th><th>Positive Terrain/ Negative Terrain (0x,000)</th><th>Gully Bottom/ Non-Gully Bottom (00,x00)</th><th>Shady Slopes/Sunny Slopes (The Bottom of the Gully Is Not Divided) (00,0x0)</th></tr>
<tr><td rowspan="10">Slope unit classification system</td><td rowspan="5">Ordinary watershed slope units 10,000</td><td rowspan="2">Ordinary watershed positive terrain slope units 11,000</td><td rowspan="2">Ordinary watershed positive terrain slope units 11,100</td><td>Ordinary watershed positive terrain sunny slope units 11,110</td></tr>
<tr><td>Ordinary watershed positive terrain shady slope units 11,120</td></tr>
<tr><td rowspan="3">Ordinary watershed negative terrain slope units 12,000</td><td>Ordinary watershed negative terrain gully bottom slope units 12,200</td><td>Ordinary watershed negative terrain gully bottom slope units 12,200</td></tr>
<tr><td rowspan="2">Ordinary watershed negative terrain non-gully bottom slope units 12,100</td><td>Ordinary watershed negative terrain non-gully bottom sunny slope units 12,110</td></tr>
<tr><td>Ordinary watershed negative terrain non-gully bottom shady slope units 12,120</td></tr>
<tr><td rowspan="5">Inter-watershed slope units 20,000</td><td rowspan="2">Inter-watershed positive terrain slope units 21,000</td><td rowspan="2">Inter-watershed positive terrain slope units 21,100</td><td>Inter-watershed positive terrain sunny slope units 21,110</td></tr>
<tr><td>Inter-watershed positive terrain shady slope units 21,120</td></tr>
<tr><td rowspan="3">Inter-watershed negative terrain slope units 22,000</td><td>Inter-watershed positive terrain gully bottom slope units 22,200</td><td>Inter-watershed positive terrain gully bottom slope units 22,200</td></tr>
<tr><td rowspan="2">Inter-watershed positive terrain non-gully bottom slope units 22,100</td><td>Inter-watershed positive terrain non-gully bottom sunny slope units 22,110</td></tr>
<tr><td>Inter-watershed positive terrain non-gully bottom shady slope units 22,120</td></tr>
</table>

2.3. Specific Ideas and Steps for CTFL Method

2.3.1. Ordinary and Inter-Watershed Division

The watershed is a complex system with characteristics that reflect a certain hierarchy. This hierarchy stems from the hierarchy of the terrain structure, i.e., the local undulations discernible at a certain scale are part of the larger undulating terrain. Therefore, the original terrain structure determines the scale of the watershed and the existence of inter-watersheds. The watershed terrain structure used in the DEM-based watershed division method determines the inevitable existence of inter-watersheds. This is because if internal gully segments exist at the current division scale, then there must be internal catchment areas that make up the inter-watershed, which ultimately forms two types of sub-watersheds: One type of watershed is an ordinary (or complete) watershed consisting entirely of external catchments, and the other is an inter-domain area or "inter-watershed", which is composed of internal catchments that surround the same internal gully segment. Regarding the classification of slope units, the slope units of an ordinary watershed have their own hydrographic features, whereas the slope units of an inter-watershed exist within the internal catchment of a watercourse, forming slope units with distinct terrain meanings and properties in many disciplines, such as geomorphology, hydrology, and ecology [37,38]. A diagram of the ordinary and inter-domain watersheds is shown in Figure 3.

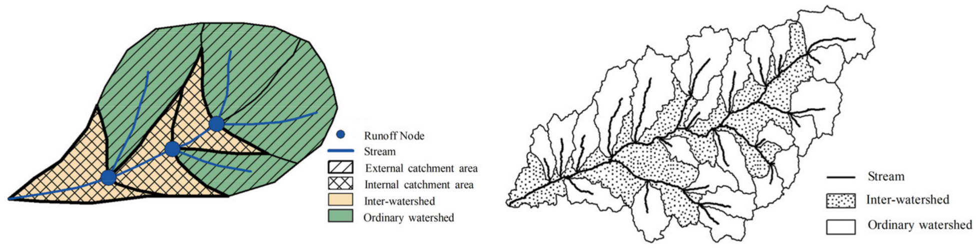

Figure 3. The diagram of the ordinary and inter-watersheds (this figure is cited from [39]).

The steps for extracting the ordinary watershed and inter-watershed are as follows: (1) First, calculate the flow accumulation. Sinks (holes) in the original DEM data were filled, and the flow directions and flow accumulation raster were calculated from the sink-free DEM using the fill, flow direction, and flow accumulation tools. (2) Then, extract the stream network. The stream network is extracted on the basis of the flow accumulation raster by setting the flow accumulation threshold using the raster calculator tool. (3) Using the Strahler method in the stream order tool, the extracted stream network is graded and coded. (4) To classify the stream network, each segment of the graded stream network is assigned a unique attribute value. (5) For automatic watershed classification, the flow direction data and the stream order data are used to extract the watershed area using the watershed tool. From this, the result of the watershed classification is obtained, which includes both inter-watershed and ordinary watersheds. The process for watershed extraction is shown in Figure 4:

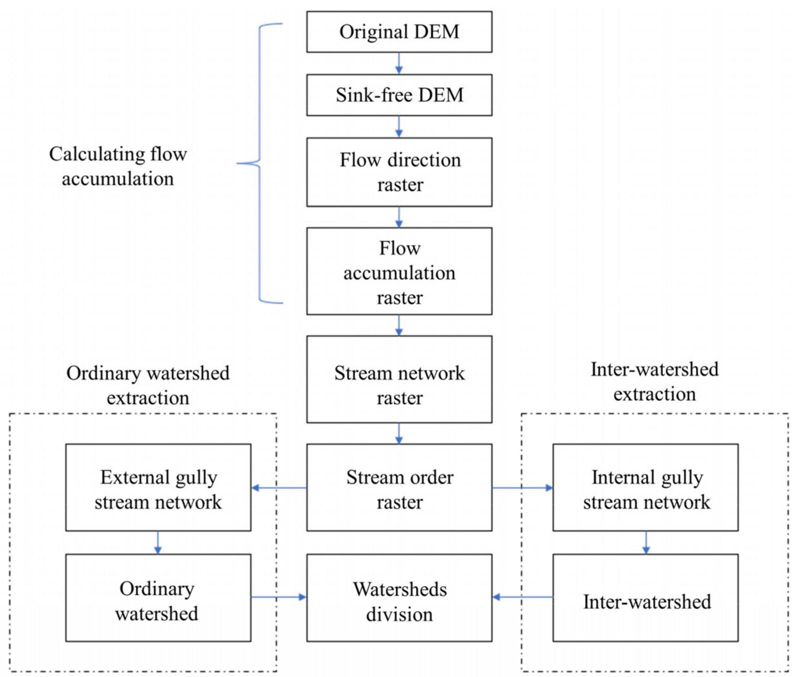

Figure 4. The process for watershed extraction.

When setting flow accumulation thresholds for stream network extraction, the arbitrary selection of different flow accumulation thresholds for the same catchment will result in different stream networks. Determining reasonable extraction thresholds is of great significance for the analysis of DEM-based watershed geomorphological characterization and the calculation of production sinks, as well as for the determination of regional ordinary watersheds/inter-watersheds [40,41]. Therefore, this paper draws on a synthesis of previous studies to extract stream networks under different flow accumulation thresholds using a trial-and-error manner before fitting the corresponding flow accumulation threshold–stream network density curves. It is shown that when the flow accumulation threshold reaches a certain value, it can be assumed that all the slope land network chains (not the actual stream network) disappear and the change in stream network density tends to flatten out, which can be used to determine a more appropriate extraction threshold and thus ensure the accuracy of the extracted ordinary watershed/inter-watershed.

2.3.2. Positive and Negative Terrain Division

The valley shoulder line is the dividing line between positive and negative terrain, and the concept of positive and negative terrain has been around for a long time. It is difficult to identify the academic literature that first proposed the concept, but the current accepted definition is that positive terrain is terrain that is relatively higher than its neighbors or is in areas of high neotectonic uplift. Mountains, plateaus, and hills are all positive terrain [42]. Conversely, negative terrain is terrain that is relatively lower than its neighbors or is an area of neotectonic subsidence. Sinks and basins are all types of negative terrain. Research has shown that positive and negative terrain is an important trait when describing geomorphic processes, and that it is also indicative of the spatial distribution of different geomorphic types. Positive and negative terrain play different roles in the material and energy transport processes of different landform areas, resulting in significant differences in terrain structure, erosion patterns, land use, and evolutionary patterns that have an impact on local human activities [43]. In this article, there are two reasons for using positive and negative terrain as the basis for the classification of slope units: First, positive and negative terrains have certain geological implications, and the positive and negative classifications of slope units, representing slope units on different surficial slopes, can increase the scientificity and rationality of the criteria for the classification. Second, positive and negative terrains have an obvious influence on human production and living activities, and the inclusion of this index will enable the results of the slope unit classification to be better used for the analysis and guidance of various production and living activities. The diagram of positive and negative terrains is shown in Figure 5.

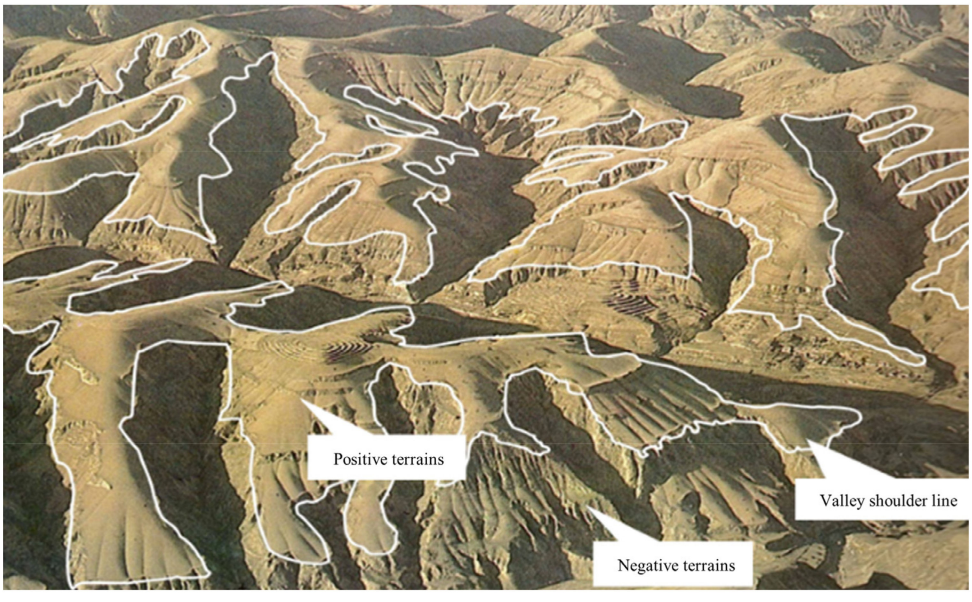

Figure 5. The diagram of positive and negative terrains (this figure is cited from [44]).

The steps to extract positive and negative terrain are based on ArcGIS software. First, apply the focal statistic tool to the original DEM data. The statistic type is mean, and the size of the neighborhood is 25 × 25 for the tool in our case. The window size is flexible according to your application and analysis scale. Hence, a smoothed terrain surface, or mean DEM, generated by the mean filter is obtained. Second, make a minus operator between the original DEM and the mean DEM in the raster calculator tool to produce the difference DEM. Third, reclassify the difference DEM by the positive and negative values to finally generate the positive and negative terrain classification results. The extraction of the positive and negative terrain based on DEM data and the corresponding process are shown in Figure 6 [45].

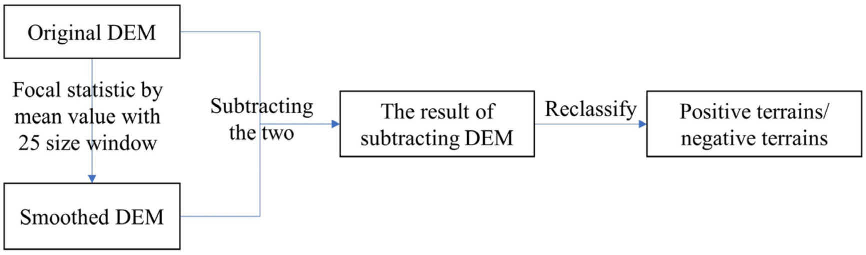

Figure 6. The process for positive and negative terrain divisions.

2.3.3. Gully Bottom and Non-Gully Bottom Division

Another type of slope land within the slope land resources is the area at the bottom of the stream/gully, called gully bottom land. Gully bottom land is distributed in narrow strips at the bottom of the gully and is an area where eroded soil material from the upper portion of the gully, which experiences little erosion, is deposited and accumulates. On gully plateaus and gully dams, the ground slope gradient is often less than 3° [46], and this type of slope land is the basis of land use in mountainous areas, the boundary line of which is divided by the slope toe line. If a mountain is considered a pyramid, the horizontal line where the pyramid intersects the ground is called the slope toe line, and the sloped edge of the pyramid is called the side slope line. The slope toe line can generally be divided by the slope gradient. The slope gradient is a quantitative description of the degree of inclination of the ground and is a basic indicator of the morphology of the landscape. The slope gradient affects the occurrence and intensity of surface runoff and soil erosion and the deployment of soil and water conservation measures by providing a surface for gravity-driven flow [47,48]. For distributed hydrological and soil erosion models at large and medium catchments and regional scales, the slope gradient is the most fundamental model parameter [49]. The diagram of the division of the valley shoulder line and the slope toe line is shown in Figure 7.

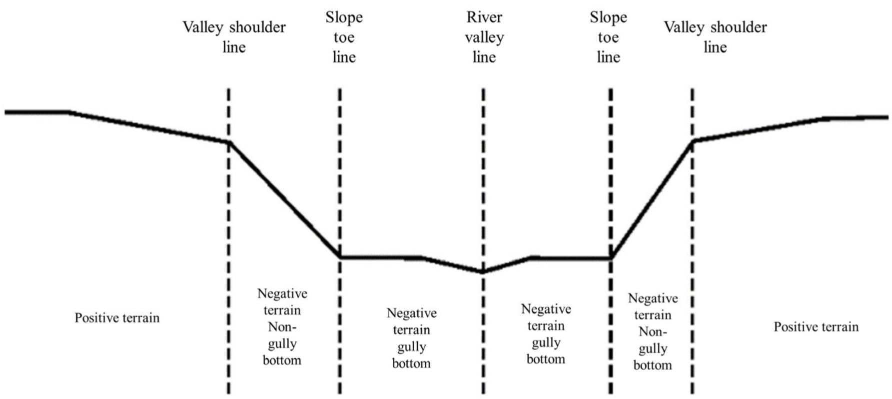

Figure 7. The diagram of the valley shoulder line and the slope toe line division.

Since the gully bottom land divided by the slope toe line is located in the negative terrain area, i.e., in the negative terrain slope unit, in this study, the negative terrain (slope ≤ 3°) was reclassified by the slope tool, and the classification results were overlaid with the stream network for analysis. The result obtained can be divided into gully bottom slope units and non-gully bottom slope units. The corresponding process is shown in Figure 8.

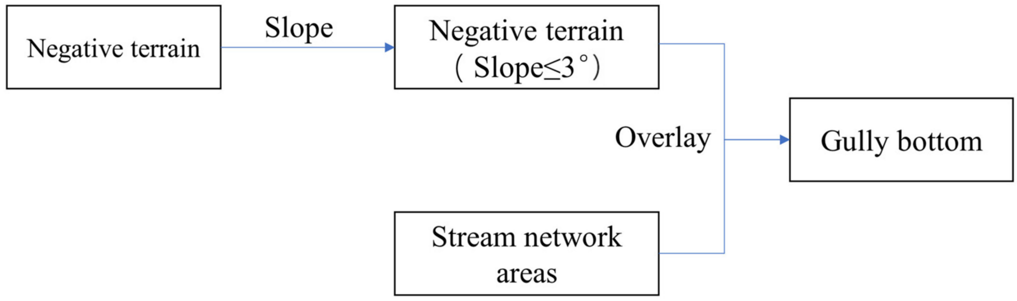

Figure 8. The process for gully bottom extraction.

2.3.4. Shady and Sunny Slope Division

In the classification of slope land, aspect should be taken into account. Aspect is the direction in which a slope faces and is the basic terrain factor describing the morphology of the ground surface. Aspect directly determines the difference in the amount of solar radiation received by the slope surface, which in turn affects the temperature, soil moisture, soil temperature, and humidity on different slopes [50,51]. The climatic differences between the different slopes provide different degrees of constraint on the other physiographic components, giving these components certain natural characteristics and, in turn, influencing the landscape and climate [52]. This complex interrelationship and interaction create the combined natural characteristics of shady and sunny slopes and exhibit marked differences and diversity. The influence of aspect-to-climate differences on the various physiographic components is manifested in the vegetation, soils, hydrology, and geomorphology. Vegetation types, soil nutrients, surface runoff, and land use vary markedly from one aspect to another. Therefore, aspect should be taken into account in the classification process of sloping land. The result of the slope units is divided into shady and sunny slopes by means of the light exposure characteristics of the slope. The diagram of the aspect algorithm is shown in Figure 9.

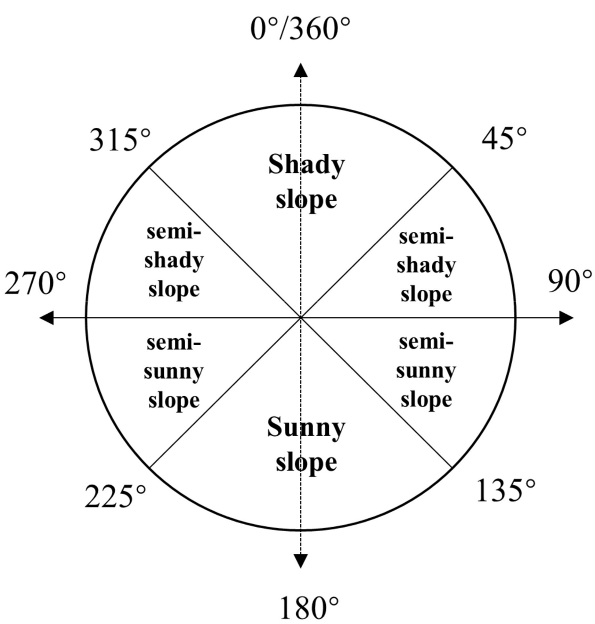

Figure 9. The diagram of aspect algorithm.

In this paper, the aspect tool within the ArcGIS software package was used to process the aspect of the original DEM, and then the results were reclassified to obtain the shady and sunny slope units.

Finally, each divided layer was overlaid according to Tables 1 and 2, some unreasonable slope units were corrected, and the final layer obtained was the map of slope unit divided by the CTFL method.

2.4. The Use of Standard Deviation for Results Evaluation

The slope unit is a kind of mapping unit divided by feature lines, and the homogeneity within the unit is required to be very high. Standard deviation is an important indicator of the dispersion of a set of data from the mean, and it is usually designed as:

$$\sigma = \sqrt{\frac{\sum_{i=1}^{n}(x_i - \mu)^2}{n}} \tag{1}$$

where x_i is the value of the i-th data, and μ is the mean [53].

Slope and aspect are two very important terrain parameters on the Earth's surface. The smaller standard deviation of slope and aspect in a slope unit indicates a lower amplitude of variation in the parameters and less distortion. Therefore, to evaluate the performance of the CTFL method, slope and aspect standard deviation were used to compare the slope unit extraction results between the CTFL method and the hydrological method. Note that the calculations of the standard deviation of slope and aspect data should use circular statistics instead of linear statistics because slope and aspect have directional properties [47].

3. Results

Slope Unit Classification for the Study Area

To select the best flow accumulation threshold when extracting the river network, a total of 13 sets of data from 500 to 40,000 threshold grids were selected in the Jiuyuangou and Lushan study areas. These were then used to calculate the corresponding stream network density from the digital water system under different critical catchment area values (Table 3) and to create the relationship curve between river network density and critical catchment area. The total length of stream network and stream network density decrease with the increase in the critical catchment area, and the extracted stream network information is more stable when the change rate of the stream network density tends to be stable. Therefore, the best flow accumulation threshold for extracting stream network information can be obtained by analyzing the relationship between the change rate of the stream network density and the critical catchment area. The threshold of the inflection point, where the slope of this curve tends to stabilize, is the critical catchment area for the development of the stream network geomorphology within the catchment, i.e., the catchment area threshold.

The relationship curve between stream network density and the critical catchment area is shown in Figure 10. The curve gradually stabilized with the increase in the number of grids. For the Jiuyuangou study area, the slope of the curve changed more when the catchment grids were in the range of 500–8000, and the slope of the curve stabilized after 8000 grids. Similarly, for the Lushan study area, the slope of the curve varied more when the catchment area was between 500 and 6000, and the slope of the curve tended to stabilize after 6000 grids were used. Therefore, in this paper, the optimal catchment area threshold was considered to be 8000 for the number of catchment grids in the Jiuyuangou study area and 6000 for the catchment area in the Lushan study area. We first extracted the general catchment and inter-watershed in the study area based on the optimal catchment area threshold. Then, the positive and negative terrains in the area were divided based on the valley shoulder line. Based on this, since the slope gradient of the gully bottom is $\leq 3^\circ$ in general, the area with slope ≤ 3 in negative terrain was extracted with slope = 3 as the slope gradient threshold, and the obtained results were overlaid with the stream network areas to obtain the gully bottom. In addition, according to the aspect tool and the reclassify tool, the shady and sunny slope units in the area can be extracted effectively. Finally, the results of the watershed/inter-watershed layer, positive/negative terrain layer, gully bottom/non-gully bottom layer, and shady/sunny slope layer were overlaid, and some unreasonable slope units were corrected. Then, the related attributes were obtained according to the location, and the slope unit classification result was obtained after coding and combining the attribute values (Figure 11).

Table 3. Calculation of the density of the stream network.

Jiuyuangou Study Area			Lushan Study Area		
Threshold	**Total Length of Stream Network/km**	**Stream Network Density/km^{-1}**	**Threshold**	**Total Length of Stream Network/km**	**Stream Network Density/km^{-1}**
500	511.910	5.301	500	4153.551	7.106
1000	392.220	4.082	1000	2780.152	4.769
2000	291.621	3.050	2000	1980.659	3.413
4000	203.800	2.156	4000	1405.358	2.447
6000	165.075	1.767	6000	1151.702	2.005
8000	139.222	1.499	8000	999.489	1.745
10,000	121.995	1.322	10,000	891.717	1.561
15,000	95.661	1.044	15,000	733.496	1.298
20,000	83.167	0.912	20,000	639.255	1.137
30,000	68.030	0.752	30,000	567.232	1.016
35,000	62.486	0.690	35,000	513.549	0.925
40,000	57.689	0.651	40,000	468.561	0.850

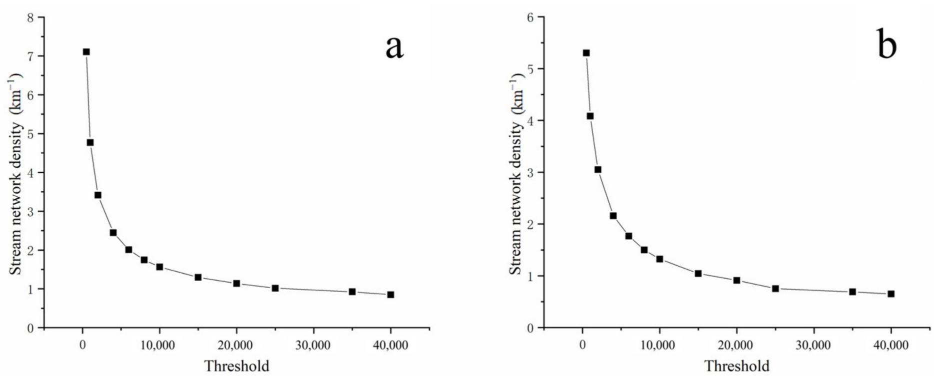

Figure 10. Relationship curve between stream network density and critical catchment area: (**a**) Jiuyuangou study area; (**b**) Lushan study area.

According to the result of the CTFL method, most of the classified slope units have strip-like shapes, which are inseparably related to the geographical structure of gullies. The combination of their boundary lines fits well with the real geographic environment and shows the topographic abruptness of the study area well. On top of that, we can clearly distinguish the slope units classified according to different terrain feature lines and the general areas where they are located, so that we can better investigate the slope land resources and prepare for the subsequent experiments and research based on them (Figure 11i,j).

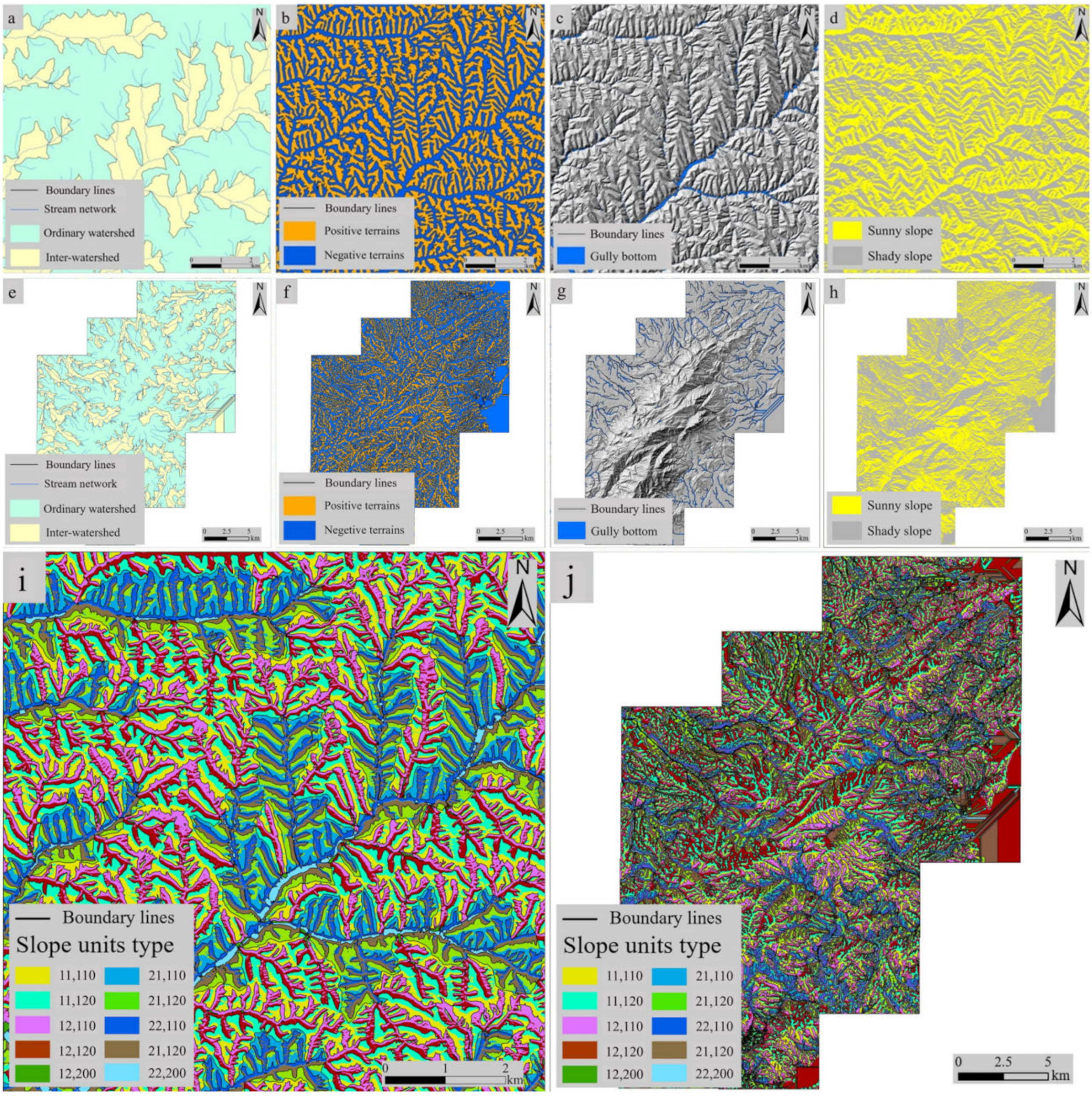

Figure 11. CTFL method process and results: (**a**) ordinary watershed and inter-watershed in Jiuyuangou, (**b**) positive terrains and negative terrains in Jiuyuangou, (**c**) non-gully bottom and gully bottom in Jiuyuangou, (**d**) positive terrains and negative terrains in Jiuyuangou, (**e**) ordinary watershed and inter-watershed in Lushan, (**f**) positive terrains and negative terrains in Lushan, (**g**) non-gully bottom and gully bottom division in Lushan, (**h**) positive terrains and negative terrains in Lushan, (**i**) the result of the CTFL method in Jiuyuangou, (**j**) the result of the CTFL method in Lushan.

4. Discussion

4.1. Significance of the CTFL Method for Sloping Land Resources

Slope land resources are important as land resources for humans, and the development and utilization of slope resources and related materials are extremely important [54]. Different kinds of slope units have various suitable land use types due to their different characteristics of slope shape, slope position, and slope nature. Unreasonable land use may not only waste slope land resources but may also contribute to the frequent occurrences of environmental hazards such as landslides, mudflows, and soil erosion [55,56]. The evaluation and planning of slope land resources by using slope units is of critical importance for the more reasonable and orderly development and utilization of these resources.

In this study, an important advantage of the slope units classified by the CTFL method compared with other slope classification methods is that CTFL not only divides the slope units, but more importantly, we categorize the slope units belonging to the same type (Table 2), which is a favorable method to investigate the land use types in the study area. We can compare the land use types of the study area and assess the slope resources of different kinds of slope units. Taking the Lushan study area as an example, we use the CTFL method to count the land use types, as shown in Figure 12. According to Figure 12, we can draw the following conclusions: for water land use types, the proportion of different slope units is similar, but the proportion of 12,200 and 22,200 slope units is less; for artificial land, the highest proportion is occupied by 12,120 type of slope units, and bare land is also similar to artificial land; for arable land, the 1x,xxx types (ordinary watershed) of slope units are significantly higher than the 2x,xxx types (inter-watershed) of slope units, and it can be concluded that the ordinary watershed has a greater proportion of arable land than the inter-watershed and that the ordinary watershed is more suitable for arable land than the inter-watershed; for forests, the proportion of slope units is higher for 11,120 and 12,120 types and smaller for the other types; and for pastures, the proportion of slope units is higher for 11,110 and 12,110 types and smaller for the other types. Compared with other slope delineation methods, the CTFL method not only fully considers the importance of geomorphology, but its delineation of slope units is also more advantageous and provides greater use.

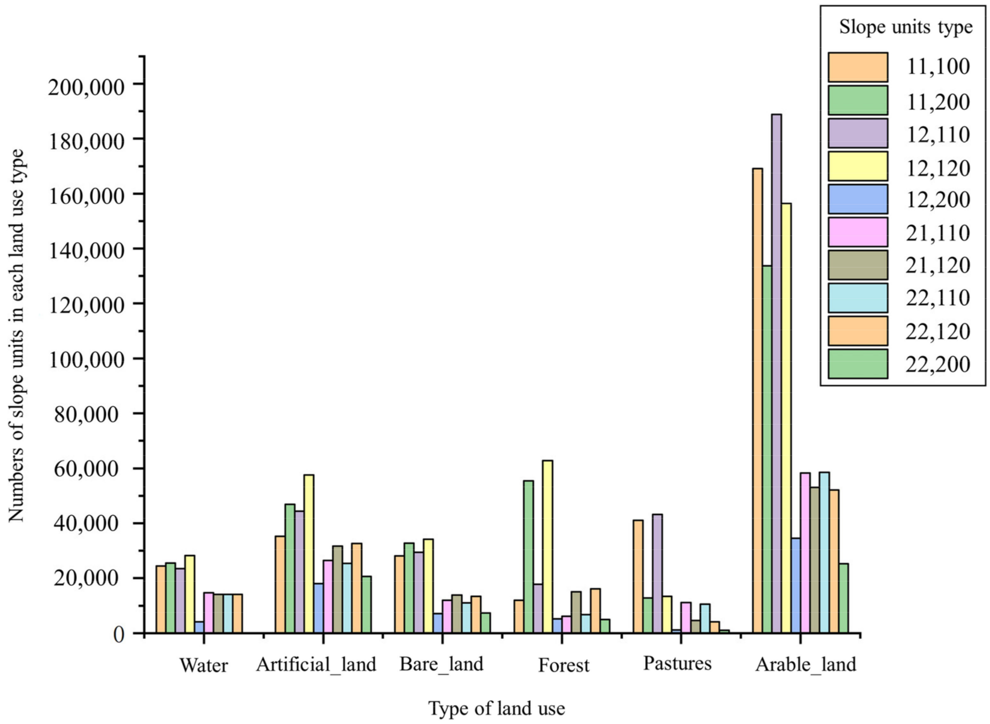

Figure 12. Histogram of the number of slope units in each land use in the Lushan area.

4.2. Use of Terrain Feature Lines in Slope Unit Classification

In previous studies, many scholars have expressed their opinions on solving the slope unit delineation problem; for example, the most common hydrological extraction method is to divide the DEM by ridgelines and valley lines in order to extract the slope units. Some scholars have also considered topography parameters, such as slope gradient and aspect, on the basis of the hydrological method. However, they more or less ignore the fact that geomorphology is a variety of spatial entities on the earth's surface in various forms, which is not an abstract combination of geometric objects but a complex geographic system of spatial properties and relationships. The division of the Earth's surface cannot be performed by mathematical calculations alone.

Terrain features form the basic framework of terrain and undulations on the ground surface, and their combination can reflect the basic shape and characteristics of terrain and landforms [57]. Therefore, to better classify the slope units, it is reasonable to take the importance of terrain feature elements into account when classifying. Because the CTFL method is based on geomorphology and not just morphology, the slope units classified are more suitable for understanding the correlation between morphological features and the composition of geomorphologic materials [58,59]. Thus, the slope units classified by this method are also more geomorphologically and physically meaningful, and the basis and results of the classification are more interpretable than the classification results obtained by other methods such as multiscale segmentation.

4.3. Comparison of Slope Unit Division between the CTFL Method and Hydrological Method

We compare the slope unit extraction results between the CTFL method and the hydrological method (Figure 13). According to Figure 13, the slope units in Figure 13b mostly cover the entire area from the top of the hill to the bottom of the gully, while the units in Figure 13a cover an area with similar properties and location, which means that the homogeneity of the slope units extracted by the CTFL method is superior to the hydrological method.

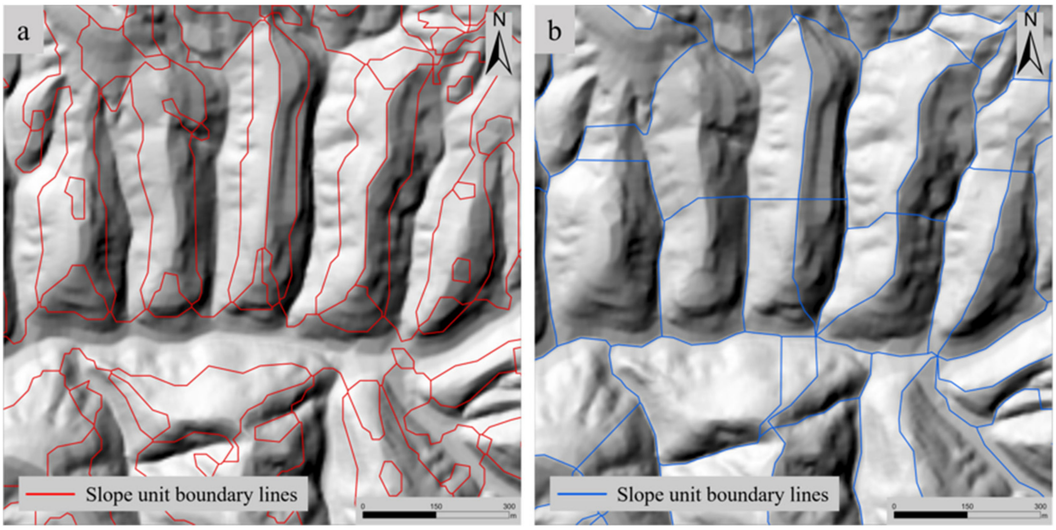

Figure 13. Slope unit extraction results: (**a**) Slope units extracted by the CTFL method; (**b**) Slope units extracted by the hydrological method.

A comparison of the slope and aspect standard deviation results is shown in Figure 14, with the slope and aspect distortion classified according to the range of slope and aspect standard deviations presented in Table 4.

The slope standard deviation results show that in the Jiuyuangou area, the average value of slope standard deviation by the CTFL method is approximately 8.51°, and the percentage of slope units with slope standard deviation between the 0 and 8° range is 42.27%, 56.21% for the 8–16° range, and 1.52% for standard deviations over 16°. The average value of slope standard deviation by the hydrological method is approximately 11.1°, and the percentage of slope units with slope standard deviation between the 0 and 8° range is 9.9%, 8–16° is 88.13%, and 3.62% for standard deviations over 16°. Similarly, in the Lushan area, the average value of slope standard deviation by the CTFL method is approximately 19.71°, and the percentage of slope units with slope standard deviation between the 0 and 8° range is 90.73%, 8.93% for the 8–16° range, and 0.34% for standard deviations over 16°. The average value of slope standard deviation by the hydrological method is approximately 24.33°, and the percentage of slope units with slope standard deviation between the 0 and 8° range is 75.33%, 8–16° is 24.24%, and 0.43% for standard deviations over 16°.

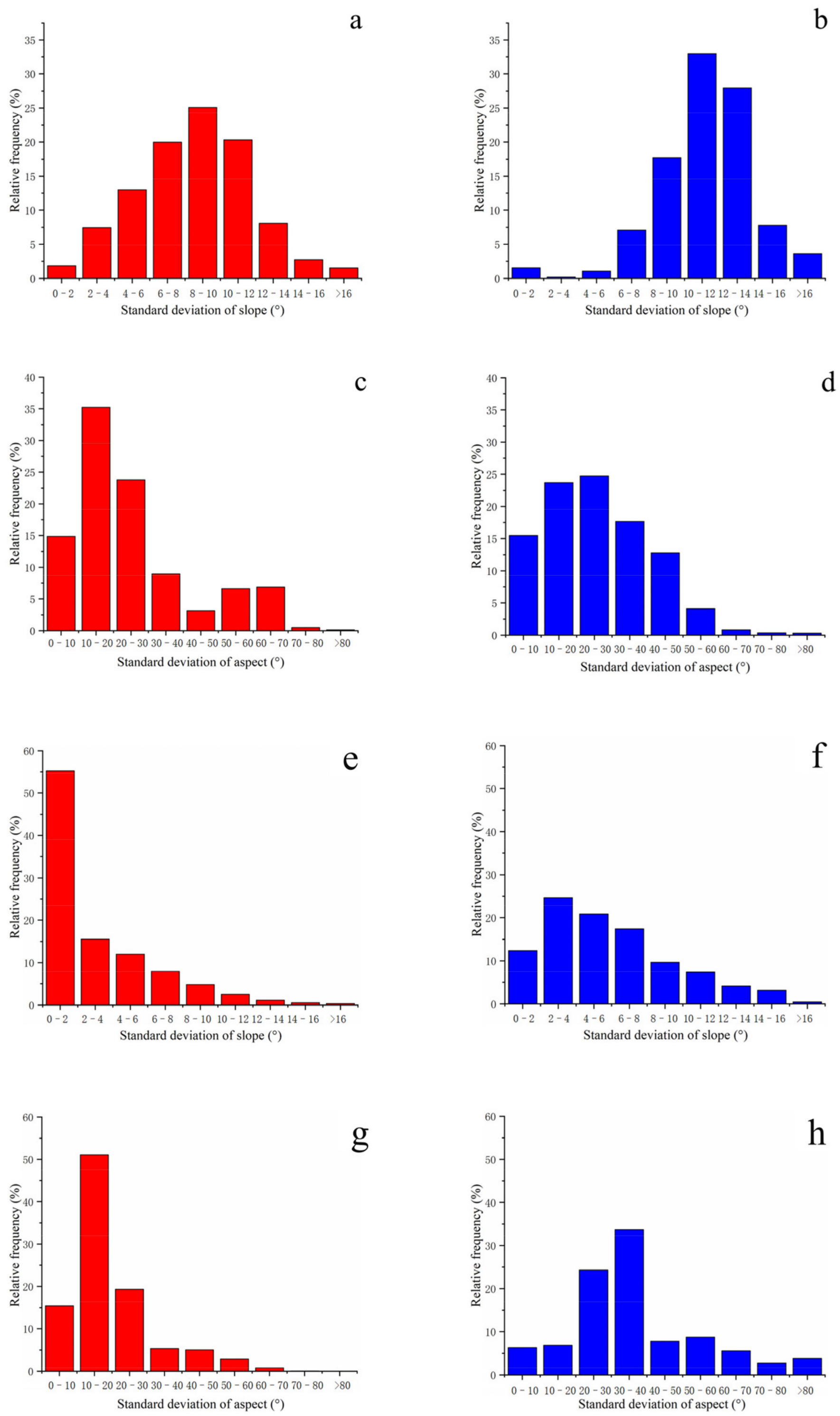

Figure 14. Comparison of slope and aspect standard deviation results: (**a**) slope standard deviation in Jiuyuangou (CTFL method); (**b**) slope standard deviation in Jiuyuangou (hydrological method); (**c**) aspect standard deviation in Jiuyuangou (CTFL method); (**d**) aspect standard deviation in Jiuyuangou (hydrological method); (**e**) slope standard deviation in Lushan (CTFL method); (**f**) slope standard deviation in Lushan (hydrological method); (**g**) aspect standard deviation in Lushan (CTFL method); (**h**) aspect standard deviation in Lushan (hydrological method).

Table 4. Classification of the degree of slope distortion and aspect distortion.

	Slope Standard Deviation Range	**0–8°**	**8–16°**	**>16°**
	Slope Distortion Classification Inside Unit	**Non-Distortion**	**Slight or Moderate Distortion**	**Severe Distortion**
Jiuyuangou area	Hydrological method (%)	9.9	86.48	3.62
	CTFL method (%)	42.27	56.21	1.52
Lushan area	Hydrological method (%)	75.33	24.24	0.43
	CTFL method (%)	90.73	8.93	0.34
	Aspect Standard Deviation Range	**0–40°**	**40–80°**	**>80°**
	Aspect Distortion Classification Inside Unit	**Non-Distortion**	**Slight or Moderate Distortion**	**Severe Distortion**
Jiuyuangou area	Hydrological method (%)	81.57	18.09	0.32
	CTFL method (%)	82.86	17.17	0.14
Lushan area	Hydrological method (%)	71.24	24.94	3.82
	CTFL method (%)	91.20	8.79	0.01

According to the aspect standard deviation results, in the Jiuyuangou area, the average value of the aspect standard deviation by the CTFL method is approximately 24.96°, and the percentage of slope units with aspect standard deviation between the 0 and 40° range is 82.86%, that of the 40–80° range is 17.17%, and 0.14% for those over 80°. The average value of the aspect standard deviation by the hydrological method is about 25.27°, and the percentage of the slope units with aspect standard deviation between the 0 and 40° range is 81.57%, that of the 40–80° range is 18.09%, and 0.32% for those above 80°. In the Lushan area, the average value of the aspect standard deviation by the CTFL method is approximately 13.58°, and the percentage of slope units with aspect standard deviation between the 0 and 40° range is 91.20%, that of the 40–80° range is 8.79%, and 0.01% for those over 80°. The average value of the aspect standard deviation by the hydrological method is approximately 31.24°, and the percentage of the slope units with aspect standard deviation between the 0 and 40° range is 71.24%, that of the 40–80° range is 24.94%, and 0.01% for those above 3.82°.

For both study areas, their slope and aspect standard deviation results indicate that the slope units extracted by CTFL have lower average values than those extracted by the hydrological method, the percentage of undistorted slope units is higher, and the percentage of severely distorted slope units is lower. Therefore, the slope units extracted by CTFL are more effective.

In a word, both from qualitative and quantitative perspectives, the CTFL method is better than the hydrological method.

4.4. Uncertainty and Future Improvement of the CTFL Method

The topographic relief highly affects the accuracy of the proposed CTFL method. The complexity and heterogeneity of the rugged land surface are shown in the intense changes in topographic characteristics, which lead to the difference in slope units in different regions. The accuracy of the algorithm is related to the quality of the extraction of the terrain features, such as ridges and valleys. Hence, the CTFL method is more suitable for terrain areas with complex structures than gentle relief regions. This leads to the different adaptabilities of the CTFL method to different landscape types [60]. It was confirmed in Section 4.3 that the slope units in the Lushan region have a better and more significant effect and higher accuracy than the slope units in the Jiuyuangou area.

Moreover, the parameter sensitivity for the extraction of terrain feature lines is difficult to avoid, and will eventually lead to differences in the accuracy of the CTFL method, such as the flow accumulation thresholds in extracting watersheds (Figure 15), the window size in extracting positive and negative terrains, etc. In this paper, the trial-and-error manner has been used to determine the input parameter values by running many parameter combinations of the input parameter values. In future improvements of the CTFL method, it will be necessary to adopt a more efficient way to determine the parameter values.

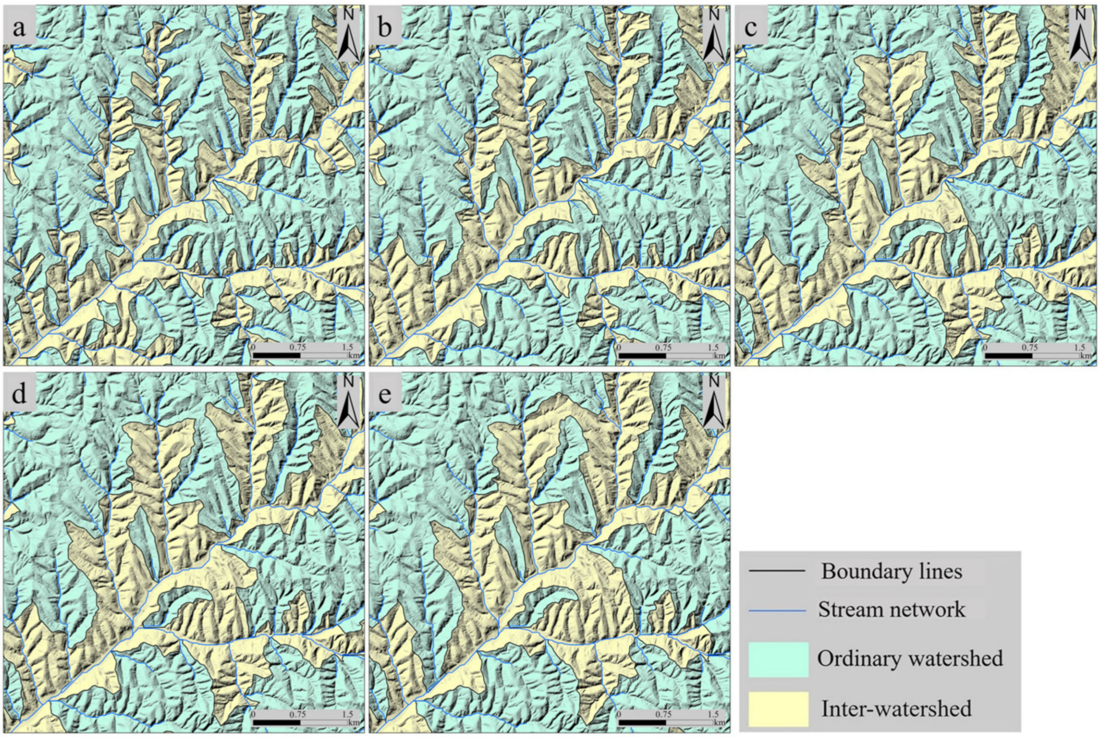

Figure 15. Extraction results for different flow accumulation thresholds for watersheds in Jiuyuangou: (**a**) extraction result when the threshold is 4000; (**b**) extraction result when the threshold is 6000; (**c**) extraction result when the threshold is 8000; (**d**) extraction result when the threshold is 10,000; (**e**) extraction result when the threshold is 12,000.

There are many other terrain features on the Earth's surface besides the geomorphic water dividing lines, such as the valley shoulder lines, the slope toe lines, and shady/sunny slope boundary lines. Some areas may not have some of these four terrain feature lines. The potential for improvement is making some corrections and additions to a specific landform. For example, the agricultural terrace lines in the anthropogenic landforms.

5. Conclusions

In this research, we proposed a slope unit classification method by combining terrain feature lines (CTFL method). This was accomplished by first dividing the slope surface into the ordinary watershed and inter-watershed along geomorphic watershed lines, then by dividing the slope surface into positive and negative terrain slope units and gully/non-gully bottom slope units according to the valley shoulder lines and slope toe lines. Finally, we divided the slope units by the shady/sunny slope boundary lines. This method discards the previous thinking of geometric division, which mainly considered topographic attributes when dividing slope units and reconsiders the importance of geomorphology. This is a new way of thinking when dividing slope units. In addition, the comparison between the

CTFL method and the hydrological method in this paper shows that the CTFL method is better than the hydrological method, and the distortion of slope units is significantly lower than that of the hydrological method in terms of both slope gradient and aspect. Future improvements to this method will focus on experimenting with other types of landform areas to determine the applicability of the method. Moreover, there are some subjective factors taken into account in the classification of slope units, which will be replaced by a more rational mode in the future to increase the robustness of the method.

Author Contributions: Conceptualization, G.T. and L.X; methodology, H.W. (Hao Wang), G.H., J.M., H.W. (Hong Wei) and S.L.; validation, H.W. (Hao Wang), G.H., J.M., H.W. (Hong Wei) and S.L.; writing—original draft preparation, H.W. (Hao Wang), G.H., J.M., H.W. (Hong Wei) and S.L.; writing—review and editing, H.W. (Hao Wang), G.T. and L.X.; supervision, G.T.; funding acquisition, G.T. All authors have read and agreed to the published version of the manuscript.

Funding: This work was supported by the National Natural Science Foundation of China [grant numbers: No. 41930102 and No. 41971333]; and the Priority Academic Program Development of Jiangsu Higher Education Institutions.

Institutional Review Board Statement: Not applicable.

Informed Consent Statement: Not applicable.

Data Availability Statement: Data will be made available on reasonable request.

Conflicts of Interest: The authors declare no conflict of interest.

References

1. Xiong, L.; Li, S.; Hu, G.; Wang, K.; Chen, M.; Zhu, A.; Tang, G. Past rainfall-driven erosion on the Chinese loess plateau inferred from archaeological evidence from Wucheng City, Shanxi. *Commun. Earth Environ.* **2023**, *4*, 4. [CrossRef]
2. Guzzetti, F.; Peruccacci, S.; Rossi, M.; Stark, C.P. Rainfall thresholds for the initiation of landslides in central and southern Europe. *Meteorol. Atmos. Phys.* **2007**, *98*, 239–267. [CrossRef]
3. Kanungo, D.P.; Sharma, S. Rainfall thresholds for prediction of shallow landslides around Chamoli-Joshimath region, Garhwal Himalayas, India. *Landslides* **2014**, *11*, 629–638. [CrossRef]
4. Wei, F.Q.; Gao, K.C.; Jiang, Y.H.; Jia, S.W.; Cui, P.; Xu, J.; Bi, B.G. GIS-based prediction of debris flows and landslides in Southwestern China. In Proceedings of the 4th International Conference on Debris-Flow Hazards Mitigation-Mechanics, Prediction, and Assessment, Chengdu, China, 10–13 September 2007; Volume 9, pp. 10–13.
5. Wang, X.; Zhang, L.; Wang, S.; Lari, S. Regional landslide susceptibility zoning with considering the aggregation of landslide points and the weights of factors. *Landslides* **2014**, *11*, 399–409. [CrossRef]
6. Salciarini, D.; Godt, J.W.; Savage, W.Z.; Conversini, P.; Baum, R.L.; Michael, J.A. Modeling regional initiation of rainfall-induced shallow landslides in the eastern Umbria Region of central Italy. *Landslides* **2006**, *3*, 181–194. [CrossRef]
7. Godt, J.W.; Schulz, W.H.; Baum, R.L.; Savage, W.Z. Modeling rainfall conditions for shallow landsliding in Seattle, Washington. *Rev. Eng. Geol.* **2008**, *20*, 137–152.
8. Michel, G.P.; Kobiyama, M.; Goerl, R.F. Comparative analysis of SHALSTAB and SINMAP for landslide susceptibility mapping in the Cunha River basin, southern Brazil. *J. Soils Sediments* **2014**, *14*, 1266–1277. [CrossRef]
9. Iverson, R.M. Landslide triggering by rain infiltration. *Water Resour. Res.* **2000**, *36*, 1897–1910. [CrossRef]
10. Xie, M.; Esaki, T.; Zhou, G. GIS-based probabilistic mapping of landslide hazard using a three-dimensional deterministic model. *Nat. Hazards* **2004**, *33*, 265–282. [CrossRef]
11. Qiu, C.; Xie, M.W.; Tetsuro, E. Landslide hazard assessment on highway slope in weathered granite zone—An example of no. 49 national highway in Hehu area, Japan. *Chin. J. Geol. Hazard Control.* **2005**, *16*, 23–28.
12. Giles, P.T.; Franklin, S.E. An automated approach to the classification of the slope units using digital data. *Geomorphology* **1998**, *21*, 251–264. [CrossRef]
13. Guzzetti, F.; Carrara, A.; Cardinali, M.; Reichenbach, P. Landslide hazard evaluation: A review of current techniques and their application in a multi-scale study, Central Italy. *Geomorphology* **1999**, *31*, 181–216. [CrossRef]
14. *Geographical Information Systems in Assessing Natural Hazards*; Springer Science + Business Media: Berlin/Heidelberg, Germany, 2013.
15. Domènech, G.; Alvioli, M.; Corominas, J. Preparing first-time slope failures hazard maps: From pixel-based to slope unit-based. *Landslides* **2020**, *17*, 249–265. [CrossRef]
16. Tanyas, H.; Rossi, M.; Alvioli, M.; van Westen, C.J.; Marchesini, I. A global slope unit-based method for the near real-time prediction of earthquake-induced landslides. *Geomorphology* **2019**, *327*, 126–146. [CrossRef]
17. Hoosbeek, M.R.; Bryant, R.B. Towards the quantitative modeling of pedogenesis—A review. *Geoderma* **1992**, *55*, 183–210. [CrossRef]

18. Hudson, B.D. The soil survey as paradigm-based science. *Soil Sci. Soc. Am. J.* **1992**, *56*, 836–841. [CrossRef]
19. Jia, N.; Mitani, Y.; Xie, M.; Djamaluddin, I. Shallow landslide hazard assessment using a three-dimensional deterministic model in a mountainous area. *Comput. Geotech.* **2012**, *45*, 1–10. [CrossRef]
20. Gruber, S.; Peckham, S. Land-surface parameters and objects in hydrology. *Dev. Soil Sci.* **2009**, *33*, 171–194.
21. Seibert, J.; McGlynn, B.L. A new triangular multiple flow direction algorithm for computing upslope areas from gridded digital elevation models. *Water Resour. Res.* **2007**, *43*, 306–320. [CrossRef]
22. Drăguţ, L.; Blaschke, T. Automated classification of landform elements using object-based image analysis. *Geomorphology* **2006**, *81*, 330–344. [CrossRef]
23. Van Asselen, S.; Seijmonsbergen, A.C. Expert-driven semi-automated geomorphological mapping for a mountainous area using a laser DTM. *Geomorphology* **2006**, *78*, 309–320. [CrossRef]
24. Pennock, D.J.; Zebarth, B.J.; De Jong, E. Landform classification and soil distribution in hummocky terrain, Saskatchewan, Canada. *Geoderma* **1987**, *40*, 297–315. [CrossRef]
25. MacMillan, R.A.; Pettapiece, W.W.; Nolan, S.C.; Goddard, T.W. A generic procedure for automatically segmenting landforms into landform elements using DEMs, heuristic rules and fuzzy logic. *Fuzzy Sets Syst.* **2000**, *113*, 81–109. [CrossRef]
26. Minár, J.; Evans, I.S. Elementary forms for land surface segmentation: The theoretical basis of terrain analysis and geomorphological mapping. *Geomorphology* **2008**, *95*, 236–259. [CrossRef]
27. Brown, D.G.; Lusch, D.P.; Duda, K.A. Supervised classification of types of glaciated landscapes using digital elevation data. *Geomorphology* **1998**, *21*, 233–250. [CrossRef]
28. Ghosh, S.; Stepinski, T.; Vilalta, R. Automatic annotation of planetary surfaces with geomorphic labels. *IEEE Trans. Geosci. Remote Sens.* **2009**, *48*, 175–185. [CrossRef]
29. Huang, F.; Tao, S.; Chang, Z.; Huang, J.; Fan, X.; Jiang, S.H.; Li, W. Efficient and automatic extraction of slope units based on multi-scale segmentation method for landslide assessments. *Landslides* **2021**, *18*, 3715–3731. [CrossRef]
30. Alvioli, M.; Marchesini, I.; Reichenbach, P.; Rossi, M.; Ardizzone, F.; Fiorucci, F.; Guzzetti, F. Automatic delineation of geomorphological slope units with r. slopeunits v1. 0 and their optimization for landslide susceptibility modeling. *Geosci. Model Dev.* **2016**, *9*, 3975–3991. [CrossRef]
31. Schlögel, R.; Marchesini, I.; Alvioli, M.; Reichenbach, P.; Rossi, M.; Malet, J.P. Optimizing landslide susceptibility zonation: Effects of DEM spatial resolution and slope unit delineation on logistic regression models. *Geomorphology* **2018**, *301*, 10–20. [CrossRef]
32. Wang, K.; Zhang, S.; DelgadoTéllez, R.; Wei, F. A new slope unit extraction method for regional landslide analysis based on morphological image analysis. *Bull. Eng. Geol. Environ.* **2019**, *78*, 4139–4151. [CrossRef]
33. Walsh, S.J.; Butler, D.R.; Malanson, G.P. An overview of scale, pattern, process relationships in geomorphology: A remote sensing and GIS perspective. *Geomorphology* **1998**, *21*, 183–205. [CrossRef]
34. Romero, B.E.; Clarke, K.C. Exploring uncertainties in terrain feature extraction across multi-scale, multi-feature, and multi-method approaches for variable terrain. *Cartogr. Geogr. Inf. Sci.* **2018**, *45*, 381–399. [CrossRef]
35. Syzdykbayev, M.; Karimi, B.; Karimi, H.A. A Method for Extracting Some Key Terrain Features from Shaded Relief of Digital Terrain Models. *Remote Sens.* **2020**, *12*, 2809. [CrossRef]
36. Yang, B.; Wang, W.L.; Guo, M.M.; Guo, W.Z.; Wang, W.X.; Kang, H.L.; Chen, Z.X. Soil erosion of unpaved loess roads subjected to an extreme rainstorm event: A case study of the Jiuyuangou watershed on the Loess Plateau, China. *J. Mt. Sci.* **2019**, *16*, 1396–1407. [CrossRef]
37. Miao, C.; Ding, M. Social vulnerability assessment of geological hazards based on entropy method in Lushan earthquake-stricken area. *Arab. J. Geosci.* **2015**, *8*, 10241–10253. [CrossRef]
38. Aksoy, H.; Kavvas, M.L. A review of hillslope and watershed scale erosion and sediment transport models. *Catena* **2005**, *64*, 247–271. [CrossRef]
39. Lin, W.T.; Chou, W.C.; Lin, C.Y.; Huang, P.H.; Tsai, J.S. WinBasin: Using improved algorithms and the GIS technique for automated watershed modelling analysis from digital elevation models. *Int. J. Geogr. Inf. Sci.* **2008**, *22*, 47–69. [CrossRef]
40. Sun, J.W.; Tang, G.A. Inter-watershed and its automatic extraction based on DEM. *J. Geo-Inf. Sci.* **2013**, *15*, 871–878. [CrossRef]
41. O'Callaghan, J.F.; Mark, D.M. The extraction of drainage networks from digital elevation data. *Comput. Vis. Graph. Image Process.* **1984**, *28*, 323–344. [CrossRef]
42. Mallakpour, I.; Villarini, G. A simulation study to examine the sensitivity of the Pettitt test to detect abrupt changes in mean. *Hydrol. Sci. J.* **2016**, *61*, 245–254. [CrossRef]
43. Tang, G.A.; Xiao, C.C.; Jia, D.X. DEM based investigation of loess shoulder-line. *Geoinform. Geospat. Inf. Sci.* **2007**, *6753*, 854–865.
44. Zhou, Y.; Tang, G.A.; Wang, C.; Xiao, C.C.; Dong, Y.F.; Sun, J.L. Automatic segmentation of loess positive and negative terrains based on high resolution grid DEMs. *Sci. Geogr. Sin.* **2010**, *30*, 261–266.
45. Zhou, Y.; Tang, G.A.; Yang, X.; Xiao, C.; Zhang, Y.; Luo, M. Positive and negative terrains on northern Shaanxi Loess Plateau. *J. Geogr. Sci.* **2010**, *20*, 64–76. [CrossRef]
46. Zhou, Y.; Zhao, H.; Chen, M.; Tu, J.; Yan, L. Automatic detection of lunar craters based on DEM data with the terrain analysis method. *Planet. Space Sci.* **2018**, *160*, 1–11. [CrossRef]
47. Tang, G.; Li, F.; Liu, X.; Long, Y.; Yang, X. Research on the slope spectrum of the Loess Plateau. *Sci. China Ser. E Technol. Sci.* **2010**, *51*, 175–185. [CrossRef]

48. Hu, G.; Wang, C.; Li, S.; Dai, W.; Xiong, L.; Tang, G.; Strobl, J. Using vertices of a triangular irregular network to calculate slope and aspect. *Int. J. Geogr. Inf. Sci.* **2022**, *36*, 382–404. [CrossRef]
49. Hu, G.; Xiong, L.; Lu, S.; Chen, J.; Li, S.; Tang, G.; Strobl, J. Mathematical vector framework for gravity-specific land surface curvatures calculation from triangulated irregular networks. *GIScience Remote Sens.* **2022**, *59*, 590–608. [CrossRef]
50. Li, X.; Wang, G.; Li, R. A DEM based method for extraction of valley shoulder line and slope heel line. *Bull. Soil Water Conserv.* **2008**, *28*, 69–72. [CrossRef]
51. Stage, A.R.; Salas, C. Interactions of elevation, aspect, and slope in models of forest species composition and productivity. *For. Sci.* **2007**, *53*, 486–492.
52. Hu, G.; Dai, W.; Li, S.; Xiong, L.; Tang, G.; Strobl, J. Quantification of terrain plan concavity and convexity using aspect vectors from digital elevation models. *Geomorphology* **2021**, *375*, 107553. [CrossRef]
53. Sternberg, M.; Shoshany, M. Influence of slope aspect on Mediterranean woody formations: Comparison of a semiarid and an arid site in Israel. *Ecol. Res.* **2001**, *16*, 335–345. [CrossRef]
54. Lee, D.; In, J.; Lee, S. Standard deviation and standard error of the mean. *Korean J. Anesthesiol.* **2015**, *68*, 220–223. [CrossRef]
55. Moges, A.; Holden, N.M. Soil fertility in relation to slope position and agricultural land use: A case study of Umbulo catchment in southern Ethiopia. *Environ. Manag.* **2008**, *42*, 753–763. [CrossRef]
56. Evans, I.S.; Hengl, T.; Gorsevski, P. Applications in geomorphology. *Dev. Soil Sci.* **2009**, *33*, 497–525.
57. Fu, J.X.; Cao, G.C.; Guo, W.J. Land use change and its driving force on the southern slope of Qilian Mountains from 1980 to 2018. *Ying Yong Sheng Tai Xue Bao J. Appl. Ecol.* **2020**, *31*, 2699–2709. [CrossRef]
58. Xiong, L.; Li, S.; Tang, G.; Strobl, J. Geomorphometry and terrain analysis: Data, methods, platforms and applications. *Earth-Sci. Rev.* **2022**, *233*, 104191. [CrossRef]
59. De Waele, J.; Gutiérrez, F.; Parise, M.; Plan, L. Geomorphology and natural hazards in karst areas: A review. *Geomorphology* **2011**, *134*, 1–8. [CrossRef]
60. Li, S.; Li, K.; Xiong, L.; Tang, G. Generating Terrain Data for Geomorphological Analysis by Integrating Topographical Features and Conditional Generative Adversarial Networks. *Remote Sens.* **2022**, *14*, 1166. [CrossRef]